DOI: 10.1002/adfm.200600907

Using Molecular Force to Overcome Steric Barriers in a Springlike Molecular Ouroboros**

By *Sune Nygaard*, *Yi Liu*, *Paul C. Stein*, *Amar H. Flood*,* and *Jan O. Jeppesen**

A mechanically interlocked and self-complexing molecular ouroboros that incorporates the π-electron-rich monopyrrolotetrathiafulvalene (MPTTF) unit and the π-electron-poor tetracationic macrocycle cyclobis(paraquat-*p*-phenylene) ($CBPQT^{4+}$) has been synthesized and characterized. The molecular ouroboros constitutes an interesting class of redox-active interlocked molecules that is structurally similar to the image of the Serpent biting its own tail, whereas, and towards advanced functionality, its mode of action resembles a wound spring. Electrochemical methods and short timescale UV-vis-NIR (NIR: near IR) chemical switching experiments verified the reversible oxidation and reduction of the molecular ouroboros akin to the build-up and release of tension in a spring. Building out from this concept, it was determined by the time evolution of the ^{1}H NMR and UV-vis-NIR spectra, however, that the initially interlocked molecular ouroboros is converted into a linear non-interlocked state by the employment of an appropriate oxidation–reduction cycle. The oxidation-induced dethreading process occurs when the dicationic $MPTTF^{2+}$ unit is kept within close proximity to the $CBPQT^{4+}$ ring by the circular interlocked structure in order to maintain the electrostatic repulsive force between the $MPTTF^{2+}$ unit and the $CBPQT^{4+}$ ring for longer periods of time. The resulting high-energy, and now tightly wound, interlocked conformation overcomes a steric barrier in many minutes, relaxing thermodynamically to form the lowest-energy linear state in an irreversible process that would otherwise be kinetically improbable without the oxidation.

1. Introduction

Molecular machines[1] and motors[2] are being considered as miniaturized forms of their macroscopic counterparts. The potential technological applications for these systems are being actively evaluated using *biological* systems in terms of active transport and assembly.[3] These developments are based on their known performance as autonomous and either linear or rotary motors for which a large body of knowledge has been built up through the interplay of experiment,[2a–c,4] and theory.[5] Advances towards the synthesis, characterization, and utilization of *artificial* systems, however, are still ongoing. Of primary importance are the investigations of machines designed to utilize the physical laws of motion that emerge at nanometer-length scales while interacting in a wet chemical world and being buffeted around by random thermal motions in order to perform predictable functions. This overall goal recalls the objective of the early steam-engine pioneers to transform random thermal energy into orderly and directed work. Equally of interest to chemists is an ongoing exploration of molecular systems whose structures look like the familiar functioning devices of our world. For the purpose of *function*, we are borrowing the concepts and theories that have been developed for biophysics to define the design principles[5] behind controlled movements at molecular-length scales and, in particular, how thermal energy is utilized after breaking the intrinsic Boltzmann balance, that is, molecular switching,[2h,i] as a means to promote orderly directed motion—the basis for work.

In order to explore some of these themes, catenanes,[6] rotaxanes,[7] and other mechanically interlocked molecules[8] have served as ideal systems on account of the fact that they primarily define one internal coordinate along which motion can propagate. For our purposes, these studies are focused on a well-characterized redox-driven motion of a tetracationic π-electron-deficient ring,[9] cyclobis(paraquat-*p*-phenylene) ($CBPQT^{4+}$), either around or along a single internal coordinate that is defined by a macrocycle or dumbbell, respectively. The

[*] Prof. A. H. Flood
Department of Chemistry
Indiana University
800 E. Kirkwood Avenue, Bloomington, IN 47405-7102 (USA)
E-mail: aflood@indiana.edu
Prof. J. O. Jeppesen, S. Nygaard, Prof. P. C. Stein
Department of Physics and Chemistry
University of Southern Denmark
Campusvej 55, Odense M 5230 (Denmark)
E-mail: joj@ifk.sdu.dk
Dr. Y. Liu
The Molecular Foundry
Lawrence Berkeley National Laboratory
One Cyclotron Road, Mail Stop 67R6110, Berkeley, CA 94720 (USA)

[**] This work was funded in part by a Ph.D. Scholarship from the University of Southern Denmark to S.N. and by the Danish Natural Science Research Council (SNF, project #21-03-0317) and the Danish Strategic Research Council in Denmark through the Young Researchers Program (#2117-05-0115). A.H.F. acknowledges Indiana University for support. Portions of this work were performed at the Molecular Foundry, Lawrence Berkeley National Laboratory, which is supported by the Office of Science, Office of Basic Energy Sciences of the U.S. Department of Energy under contract No. DE-AC02-05 CH11231. Supporting Information is available online from Wiley InterScience or from the author.

motion takes place from a strong[10] π-electron donor, tetrathiafulvalene[11] (TTF) to a weaker[10] π-electron donor, naphthalene (NP), and back again. In order to garner a more complete picture of these motions we measured the thermally equilibrated energy available for force production using a specifically designed, sterically locked rotaxane[12] based upon a single monopyrrolotetrathiafulvalene[13] (MPTTF) unit encircled by $CBPQT^{4+}$. Upon sequential formation of the monocation $MPTTF^{\bullet+}$ and the dication $MPTTF^{2+}$, the electrostatic repulsion of the tetracationic $CBPQT^{4+}$ ring generates 5 and 9 kcal mol^{-1} (1 kcal = 4.184 kJ) of free energy, respectively. Although these values do not directly coincide with ones obtained from dynamic force spectroscopy,[14] ≈ 65 kcal mol^{-1}, neither do the experimental conditions—the former and the latter are measured under equilibrium and nonequilibrium conditions, respectively. Towards the utilization of this free energy and the ensuing motion to generate force, a palindromic [3]rotaxane was designed[15] to display a musclelike contraction and extension when two $CBPQT^{4+}$ rings switch their inter-ring separation from 4.2 to 1.4 nm. When ~6 billion of these [3]rotaxanes are attached to the top sides of gold-coated cantilevers via a tether on the $CBPQT^{4+}$ rings, the cantilevers were observed to repetitively and controllably bend up and down. In this context, the 9 kcal mol^{-1} was cooperatively harnessed to bend against the restoring force of the cantilever (force constant $k = 0.02$ N m^{-1}) deflecting it by 35 nm, which is consistent with 10–20 pN of force generation for each of the molecular muscles. While this example demonstrates how the energy of motion was amplified to overcome the stiffness of a large micrometer-scale cantilever, we have elaborated upon a self-complexing motif[16] (Fig. 1) that uses the energy to perform work on the nanoscale.

In this study, we will describe the preparation and dynamics of a molecular ouroboros $\mathbf{1}^{4+}$. The varieties of springlike properties were characterized in solution through a combination of electrochemical techniques and both ^{1}H NMR and UV-vis-NIR spectroscopy (NIR: near IR) for both the starting and redox-switched molecular ouroboros. During these investigations, we discovered that its behavior is exemplary for illustrating both a fast timescale tension build-up and release akin to a spring, and on a slower timescale, the use of that tension, measuring ≈ 9 kcal mol^{-1}, to overcome an internal steric barrier resulting in the unwinding of the ouroboros form into a linear one.

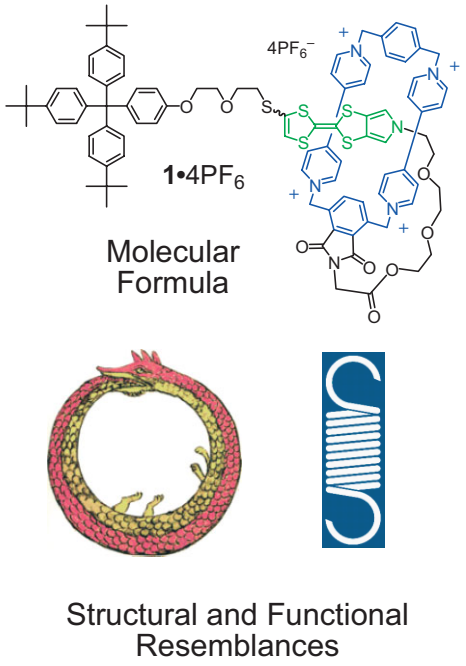

Figure 1. Structural formula of the molecular ouroboros $\mathbf{1}\cdot 4\,PF_6$, and graphical depictions of an iconic ouroboros (1478 AD) and of a functional spring.

2. Results and Discussion

2.1. Synthesis

The target compound $\mathbf{1}\cdot 4\,PF_6$ was prepared by the pathways shown in Scheme 1. A modular approach was adopted, similar to previous work[8b,17] conducted in this field of research, in which the various parts of the target molecule were prepared individually and joined covalently in the latter steps of the synthetic pathway. The MPTTF derivative **3** and the bulky, hydrophobic stopper **4** were coupled via an in situ deprotection of the cyanoethyl protection group forming the *S*-nucleophile with 1.1 equivalents of $CsOH\cdot H_2O$, to give the stoppered MPTTF derivative **5**. The tosyl protecting group on the MPTTF unit was then removed using sodium methoxide (NaOMe) in a tetrahydrofuran (THF)/methanol (MeOH) mixture with a total yield of 53 % for the two steps.

The resultant pyrrole nitrogen in **6** was alkylated with the iodo triethyleneglycol (TEG) derivative **7** in good yield (81 %) to produce **8**. Subsequent removal of the tetrahydropyran (THP) protection group on **8** with *p*-toluenesulfonic acid (TsOH) gave the alcohol **9** in 51 % yield. Esterification of **9** with the carboxylic derivative **10**, using 1,3-dicyclohexylcarbodiimide (DCC) as the coupling agent, yielded the desired dibromide **11** in 94 % yield.

The high-pressure (10 kbar, 1 bar = 10^5 Pa) reaction[18] between the dibromide **11** and the dicationic precursor $\mathbf{12}\cdot 2\,PF_6$ in dimethylformamide (DMF) at room temperature followed by counterion exchange yielded a green solid, which was found to consist mainly of the desired self-complexed cyclophane $\mathbf{1}\cdot 4\,PF_6$ together with a small fraction[19] of the noncomplexed and linear cyclophane $\mathbf{2}\cdot 4\,PF_6$ in a combined yield of 27 %. The self-complexed cyclophane $\mathbf{1}\cdot 4\,PF_6$ was isolated from the mixture by preparative thin-layer chromatography (PTLC) using acetone (Me_2CO)/NH_4PF_6 (100:1 v/w) as the eluent.[20]

2.2. Structural Characterization of the Cyclophane Structure by Mass Spectrometry

The electrospray ionization mass spectrometry (ESI-MS) investigation of $\mathbf{1}\cdot 4\,PF_6$ unambiguously confirms the presence of

ADVANCED FUNCTIONAL MATERIALS

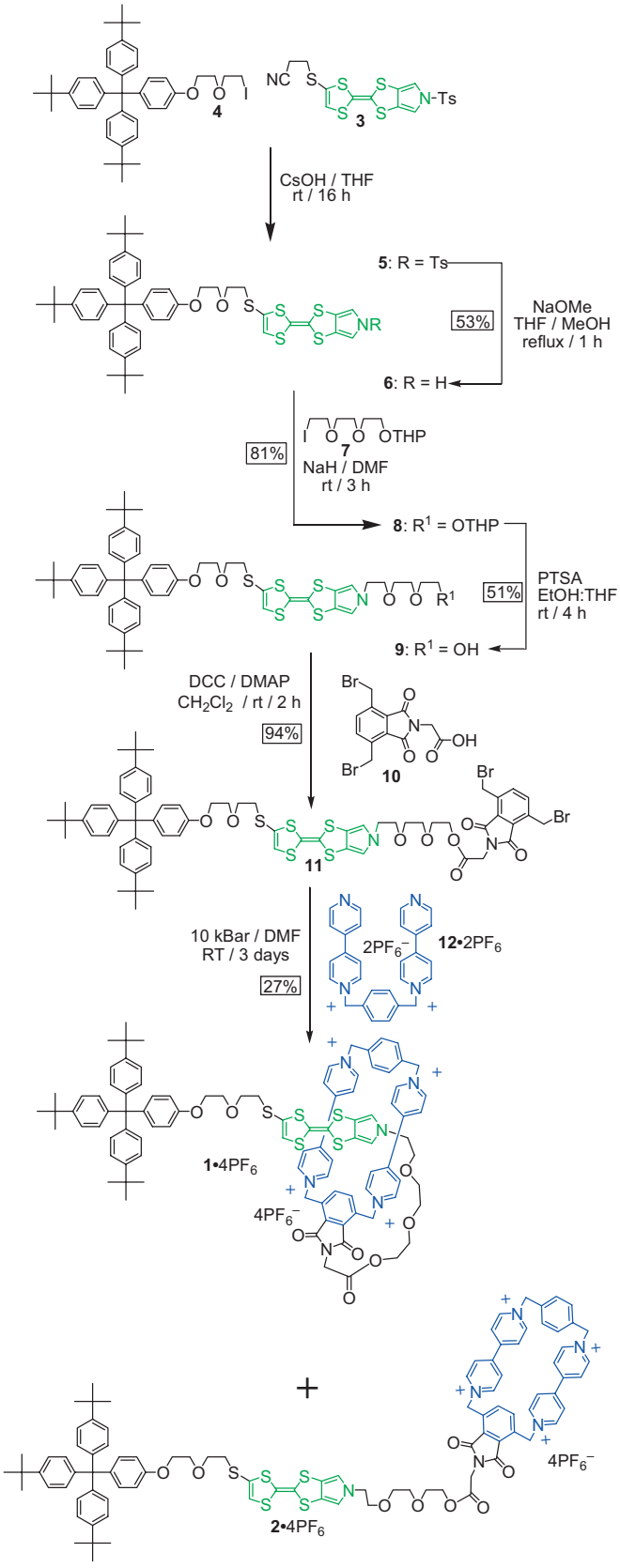

Scheme 1. Synthesis of the interlocked molecule **1**·4 PF_6 in the form of a molecular ouroboros and its linear isomer **2**·4 PF_6. All acronyms have been defined in the text.

the cyclophane structure as three indicative peaks corresponding to the loss of two, three, and four PF_6^- counterions. In particular, the quadruply charged ion $[M–4\,PF_6]^{4+}$ is seen at *m/z* 402.7, the triply charged ion $[M–3\,PF_6]^{3+}$ at *m/z* 585.2, and the doubly charged $[M–2\,PF_6]^{2+}$ at *m/z* 950.4. It is not possible to determine whether or not the isolated compound is interlocked given that the ESI-MS data is identical when comparing the mixture of **1**·4 PF_6 and **2**·4 PF_6 with the PTLC purified **1**·4 PF_6 sample. More importantly, however, no evidence was found for the formation of higher molecular weight interlocked isomers, such as structures that have been described in the past as daisy chains.[21]

2.3 Structural Characterization by ^{1}H NMR Spectroscopy

The assignment of the ^{1}H NMR spectrum of the self-complex $\mathbf{1}^{4+}$ is complicated by the need to account for the 98 protons present in the molecule, together with the fact that $\mathbf{1}^{4+}$ exhibits a dynamic behavior at room temperature. However, an investigation of the ^{1}H NMR spectrum at low temperatures indicates that $\mathbf{1}^{4+}$ exists as a mixture of two interlocked isomers. The ^{1}H NMR spectrum (500 MHz) of the interlocked compound $\mathbf{1}^{4+}$ recorded in $(CD_3)_2CO$ at 198 K (Fig. 2) displays eight signals in the downfield region (δ = 9.3–10.0 ppm), together with eight signals resonating between δ = 8.3 and δ = 9.0 ppm.

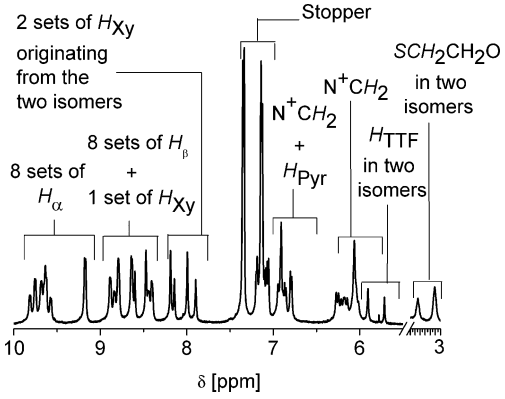

Figure 2. Downfield and upfield regions of the ^{1}H NMR spectrum ($(CD_3)_2CO$, 500 MHz) of $\mathbf{1}^{4+}$ recorded at 198 K.

Further inspection of these signals as substantiated by the analysis of the ^{1}H COSY data (correlation spectroscopy; see Supporting Information, Fig. S2) reveals that two sets of signals are present in each of the regions mentioned above, each set consisting of four signals with different relative intensities. It is well known[17] that signals in these regions, for this particular type of compound, can be associated with the resonances for the bipyridinium H_α (δ = 9.3–10.0 ppm) and H_β (δ = 8.3–9.0 ppm) protons in the $CBPQT^{4+}$ cyclophane moiety. The presence of two distinctive sets of four H_α and H_β resonances confirms the interlocked nature of the isolated compound as well as the presence of two isomers (Scheme 2). The four signals of H_α and H_β arise from a low degree of symmetry and

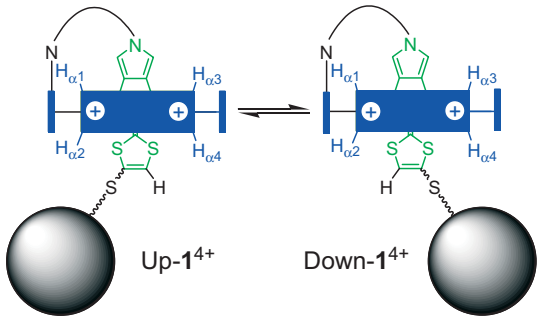

Scheme 2. The equilibrium between the two self-complexed conformations observed for $\mathbf{1}^{4+}$. The descriptor Up and Down refers to the self-complexed conformation in which H_{TTF} is pointing away from and towards the diimidophenylene ring, respectively.

the lack of free rotation in the interlocked isomers at low temperature, rendering all positions different within a single bipyridinium unit of the cyclophane. The two species are assigned[22] to two conformations that differ in the relative orientation of the MPTTF unit inside the CBPQT^{4+} cyclophane (Scheme 2).

MPTTF units are normally considered[23] to be isomer-free in mechanically interlocked [2]rotaxanes, however, the ouroboros-like steric constraints of the curved structure creates two distinct and chemically different ways for the MPTTF unit to be located inside the tetracationic cyclophane. This situation emerges when the terminal hydrogen of the MPTTF unit (H_{TTF}) is facing up and away from the diimidophenylene ring of the tetracationic cyclophane or down and into it. It is not evident from these data which conformation is favored at 198 K in $(CD_3)_2CO$, but integration of the peak areas (H_{Xy}, H_{TTF}, and SCH_2CH_2O) allow us to estimate the relative distribution of the two interlocked conformations in $\mathbf{1}^{4+}$ to be on the order of 6:4 in $(CD_3)_2CO$ at 198 K.

2.4. Dynamic ^{1}H NMR Spectroscopy

Variable-temperature (VT) ^{1}H NMR spectroscopy carried out on $\mathbf{1}^{4+}$ in $(CD_3)_2CO$ reveals that the resonances associated with the H_α and H_β bipyridinium protons (Fig. 3a) of the tetracationic cyclophane CBPQT^{4+}, as well as the SCH_2CH_2O resonances, are observed to undergo coalescence with increasing temperature. This is clearly seen for the H_α bipiridinium protons, which, as mentioned previously, are found at low temperature as 2×4 sets of well-defined signals, but coalesce into three broad signals at elevated temperature.

The coalescence phenomena is also observed for the two different types of SCH_2CH_2O protons (Fig. 3b), where it is possible at low temperature to observe two sets of signals originating from the two distinct interlocked conformations of $\mathbf{1}^{4+}$, entirely consistent with the fact that the MPTTF unit is encircled in an "up" or a "down" fashion inside the CBPQT^{4+} cyclophane. These signals coalesce into one signal at higher temperature (288 K). Exchange rates, and consequently, activation energies, can be derived[24] from the coalescence temperatures of the VT ^{1}H NMR spectra from 203–298 K (see Supporting Information). It was determined from these measurements that the free energy of activation ($\Delta G^{\ddagger}$) for the net flipping between the up and down conformations of the MPTTF unit inside the CBPQT^{4+} ring is 14 ± 3 kcal mol^{-1} at 293 K.

2.5. Photophysical Investigations

The photophysical properties have been studied in air-equilibrated acetonitrile (MeCN) or Me_2CO at room temperature. Two systems have been investigated, namely: i) the threadlike component **9** and ii) the self-complex $\mathbf{1}^{4+}$. The UV-vis-NIR spectrum (Fig. 4) of the self-complexed molecule $\mathbf{1}^{4+}$ displays a significant change in the visible to NIR region of the spectrum, where a broad and relatively weak band is observed for the self-complex at 825 nm (Me_2CO: $\varepsilon = 1100$ mol^{-1} cm^{-1}). It is well known[17,25] that such a band is typical of charge-transfer (CT) interactions arising from the encirclement of the MPTTF unit by the tetracationic cyclophane CBPQT^{4+}. The effect of the solvent on the localization of the CT band is limited.

However, an interesting observation was made during the UV-vis-NIR absorption spectroscopic investigation of $\mathbf{1}^{4+}$, namely that there is a pronounced time dependence (Fig. 5) of the absorption spectrum directly after the solid form of the self-complexed compound $\mathbf{1}\cdot4\,PF_6$ is dissolved in Me_2CO.[26] Initially a green solution with a symmetric CT band centered at 825 nm is observed. Over a period of $\approx$2500 s (see Fig. S5), however, a spectroscopic change occurs that ultimately breaks the initial symmetry of the CT band through the appearance of

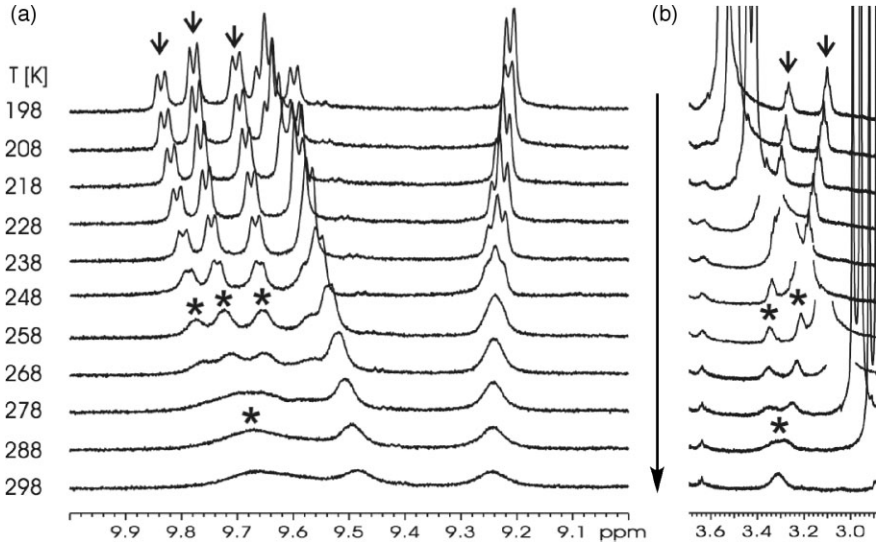

Figure 3. a) Downfield and b) upfield region of the ^{1}H NMR spectra ($(CD_3)_2CO$, 500 MHz) of $\mathbf{1}^{4+}$ recorded with increasing temperatures. The peaks that are used to determine the exchange rates are marked with arrows before coalescence and stars after coalescence.

ADVANCED FUNCTIONAL MATERIALS

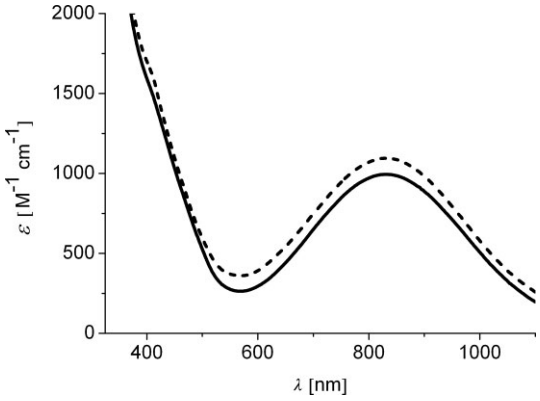

Figure 4. Comparison of the absorption spectra of $\mathbf{1}^{4+}$ recorded in MeCN (solid line) and Me_2CO (dashed line) at room temperature immediately after their dissolution.

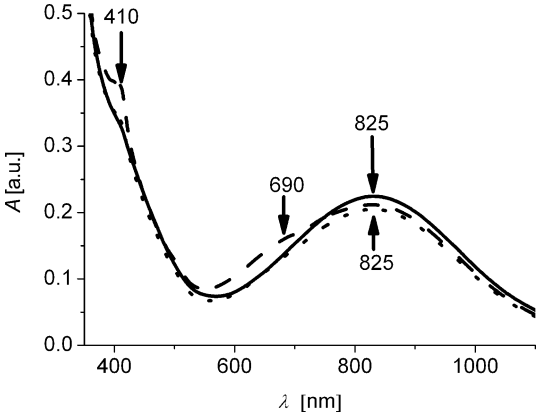

Figure 5. Absorption spectra of $\mathbf{1}^{4+}$ recorded in Me_2CO immediately after dissolving the solid compound (solid line), after 2340 s (dashed line), and after 14 400 s (dotted line).

two new absorptions centered at 690 and 410 nm. This initial spectroscopic change is followed by a second slower process lasting ≈ 4 h (see Fig. S6), during which time the two new bands disappear thereby restoring the symmetry of the 825 nm band but without the full intensity (92 %). There was no evidence of a similar tendency in MeCN.

The process is found to be entirely reversible through two cycles of dissolution, solvent removal in vacuo, and re-dissolution in Me_2CO. A subtraction of the intermediate time spectrum (dashed line in Fig. 5) from the initial one looks akin to either the $MPTTF^{\bullet+}$ or bipyridinium monocation. The assignment of these observations to either a structural reorganization or a change in the redox state was not able to be substantiated by using either ^1H NMR (structurally sensitive) or resonance Raman (electronically sensitive) spectroscopic techniques on account of the low concentration of the intermediate.

2.6. Electrochemical Investigations

The short timescale (< 10 s) redox-switching properties of the molecular ouroboros $\mathbf{1}^{4+}$ were determined using cyclic voltammetry (CV) and differential pulse voltammetry (DPV) and by comparison (Fig. 6) to the threadlike component **9**. Contrary to all other previous mechanically interlocked (MP)TTF-$CBPQT^{4+}$ systems,[6a,8b,12b,15,17b,c,e] and in particular for related self-complexing systems,[22] the oxidation of the MPTTF unit in

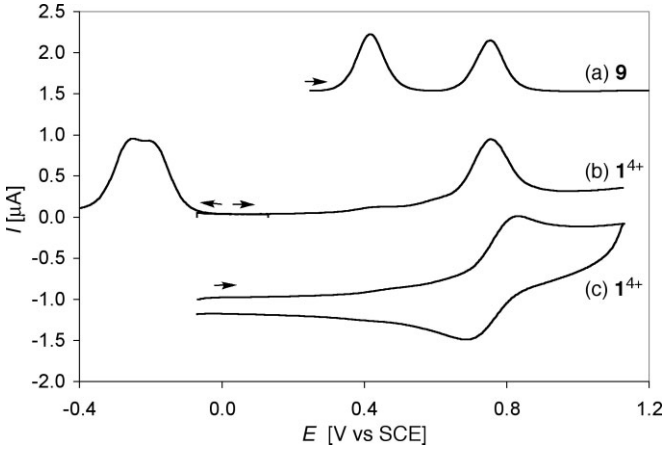

Figure 6. Electrochemical responses of the a) half-dumbbell **9** (DPV, 1 mM) compared to the b) DPV and c) CV (200 $mV s^{-1}$) of the molecular ouroboros $\mathbf{1}^{4+}$ (0.5 mM). Currents scaled (× 0.5 (a) and × 0.33 (c)) and offset for clarity. Glassy carbon working electrode, Pt counter electrode, and SCE reference electrode, 0.1 M $TBAPF_6$, MeCN, Ar degassed.

$\mathbf{1}^{4+}$ proceeds directly from the neutral form to the dication and is directly reduced back again in a seemingly simple two-electron process at an observed half-wave potential of +760 mV versus SCE (saturated calomel electrode).[27] Consistent with this interpretation, there is only the one oxidation peak observed in either the CV or DPV response up to +1.6 V.[28] The separation of the first two-electron reduction of the $CBPQT^{4+}$ ring into two peaks at about –200 mV is indicative of the interlocked character of $\mathbf{1}^{4+}$.[29] Consistent with previous investigations,[6a,12b,30] the oxidation behavior suggests that the MPTTF unit is tightly encircled right up until the potential (+760 mV) that it is oxidized to the $MPTTF^{\bullet+}$ monocation, at which point it is electrostatically and rapidly repelled out of the central cavity of the $CBPQT^{4+}$. Once outside, the $MPTTF^{2+}$ dication readily forms at the same potential as that displayed for the thread's stepwise formation of its doubly oxidized form, $\mathbf{9}^{2+}$. This coupled mechanochemical process results in the appearance of the single two-electron oxidation peak in the CV, representing the conversion from $\mathbf{1}^{4+}$ to $\mathbf{1}^{6+}$ while still maintaining the interlocked structure. The returning sweep displays a unique feature corresponding to a two-electron reduction peak indicating that the $MPTTF^{2+}$ dication is reduced directly back to the neutral $MPTTF^0$ unit. That is, while the rapid redox-driven movement of the $CBPQT^{4+}$ ring away from the oxidized $MPTTF^{\bullet+}$ monocation is typical,[6a,8b,12b,15,17b,c,e,22,30] the ring's equally rapid return has not been observed to this extent until now, on account of the fact that it is usually held both thermodynamically and kinetically apart[6d,17e,31] from the $(MP)TTF^0$ unit. These observations suggest that even though the

$CBPQT^{4+}$ ring is repelled sufficiently far away from the site of charge–charge repulsion ($MPTTF^{2+/+}$) in order to leave the second oxidation potential relatively unaffected, the ring is still sufficiently proximal to return once neutrality is reestablished. This behavior, which persisted down to scan rates of 25 $mV\,s^{-1}$, suggests that the molecular ouroboros remains, for the most part, self-complexed when the dicationic, high energy state $\mathbf{1}^{6+}$ is maintained for less than ≈ 15 s.

2.7. Chemical Oxidation of $\mathbf{1}^{4+}$ Monitored by Absorption Spectroscopy

It is well known[12] that the stepwise addition of the chemical oxidant $Fe(ClO_4)_3$ to MPTTF derivatives leads to the formation of the radical cation ($MPTTF^{\bullet+}$) followed by the generation of the dication ($MPTTF^{2+}$) and that these species are easily recognizable on account of their distinct profile in UV-vis-NIR absorption spectrum. The spectroscopic changes that accompany the *titrational addition* of $Fe(ClO_4)_3$ to the green solution of the interlocked compound $\mathbf{1}^{4+}$ in MeCN at room temperature (see Figs. S8 and S9) resembles the titrational addition of the chemical oxidant to the MPTTF model compound **13** (see Fig. S7) with the noted difference in the loss of TTF → $CBPQT^{4+}$ CT-band intensity for $\mathbf{1}^{4+}$ during the first oxidation. In particular, it is found that the addition of 1.0 equivalent of $Fe(ClO_4)_3$, thereby generating the $MPTTF^{\bullet+}$ radical cation, that is, $\mathbf{1}^{5+\bullet}$, leads to the appearance of the two distinct bands centered at 685 and 430 nm in the absorption spectrum (Fig. 7). The absorption band at 685 nm appears broadened and red-shifted by about 50 nm from the spectrum of $\mathbf{13}^{+\bullet}$ (see

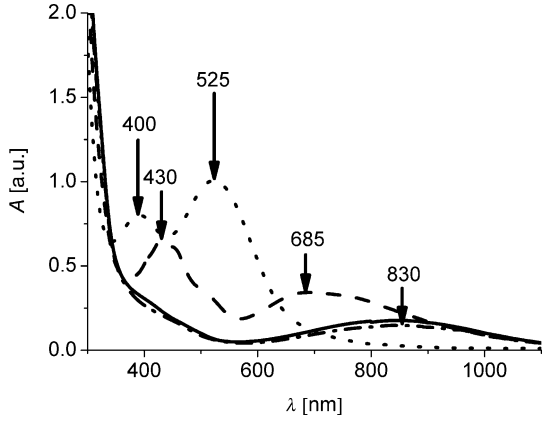

Figure 7. Overview of the spectroscopic changes after the titrational addition of 1.0 (dashed line) and 2.3 (dotted line) equivalents of $Fe(ClO_4)_3$ to a solution of $\mathbf{1}^{4+}$ in MeCN. The reduction with aqueous ascorbic acid (AA) regenerates the CT band to 85 % (dash dotted line) of its initial value (solid line).

Supporting Information). This feature might arise from an electrostatic interaction with the proximal $CBPQT^{4+}$ moiety or as a result of a new CT interaction involving the mono-oxidized $MPTTF^{\bullet+}$ unit. Addition of a second equivalent of $Fe(ClO_4)_3$ leads to the formation of the dication ($MPTTF^{2+}$), $\mathbf{1}^{6+}$, which exhibits two strong absorptions at 525 and 400 nm. The shifts in band maxima and shape between the chemically oxidized model compound $\mathbf{13}^{2+}$ and self-complexed $\mathbf{1}^{6+}$ are not as large as those observed[12] in more sterically restricted [2]rotaxanes, therefore indicating that the $CBPQT^{4+}$ ring has moved away from the cationic $MPTTF^{2+}$. The reversibility of the molecular reorganization following the oxidation process observed using CV, $\mathbf{1}^{4+} \rightleftharpoons \mathbf{1}^{6+}$, was tested by the addition of an excess of the aqueous reductant ascorbic acid (AA) and was found to regenerate the original CT band to 85 % of its initial value.

2.8. Chemical Oxidation Induced Dethreading Experiments Monitored by Absorption Spectroscopy

Although the loss of intensity for the CT band in the solution of $\mathbf{1}^{4+}$ following an oxidation–reduction cycle $\mathbf{1}^{4+} \rightleftharpoons \mathbf{1}^{6+}$ is not uncommon,[15,32] the extent of the intensity loss was larger than the usual > 90 % recovery. On the basis of this observation, we investigated the hypothesis that $\mathbf{1}^{6+}$ can lose its self-complexed structure by a dethreading process (Scheme 3) to become linear in form. In a series of oxidation–reduction experiments,[33] the $MPTTF^{2+}$ dication was generated and its spectrum measured by the addition of an *excess* of $Fe(ClO_4)_3$ (4 equiv) to a solution of the molecular ouroboros $\mathbf{1}^{4+}$ in MeCN. The redox-generated $MPTTF^{2+}$ dicationic form, $\mathbf{1}^{6+}$, was left at room temperature for different periods of time before being reduced back to its neutral form (Fig. 7). During the course of this experiment, it is important to note that the marker band for the $MPTTF^{2+}$ dication at 525 nm is virtually unaffected (see Fig. S10), indicating that the oxidized compound is stable. Addition of aqueous AA to a solution of $\mathbf{1}^{6+}$ after the increasing time periods regenerated the CT band with increasing losses of the initial intensity. Maintaining the compound in the doubly oxidized state for time periods in the range of 1800–9000 s results in a clearly visible and quantifiable decrease in the CT band after chemical reduction when compared to the original solution of $\mathbf{1}^{4+}$, and retaining the compound in the doubly oxidized state for more than 15 h prior to its reduction completely extinguished the CT band.

The loss of CT-band intensity after reduction of the MPTTF unit is assigned to the time-dependent dethreading (Scheme 3) of the interlocked compound $\mathbf{1}^{6+}$ to the corresponding linear form $\mathbf{2}^{6+}$ in the oxidized state. The barrier of the oxidation-induced dethreading of $\mathbf{1}^{6+}$ is envisioned to be imposed by the two carbonyl oxygens[34] located 0.5 nm apart (center-to-center) on the diimidophenylene ring that serves as the interconnection point between the $CBPQT^{4+}$ cyclophane moiety and the remaining half-dumbbell moiety of the molecular ouroboros. In order for the molecule to relax slowly from the intermediate high-energy conformation $\mathbf{1}^{6+}$ to the lowest energy one $\mathbf{2}^{6+}$, we suspect that when the diimidophenylene ring rotates around and within the 0.7 nm cavity (face-to-face) of the $CBPQT^{4+}$ moiety $\mathbf{1}^{6+}$, both must twist past each other in order to minimize van der Waals contact. It is by this route that the molecular ouroboros harnesses the electrostatic repulsive force and breaks free from the confines of the mechanical bond.

For this mechanism of motion to be true, the now empty $CBPQT^{4+}$ of the reduced $\mathbf{2}^{4+}$ should subsequently be available

ADVANCED FUNCTIONAL MATERIALS

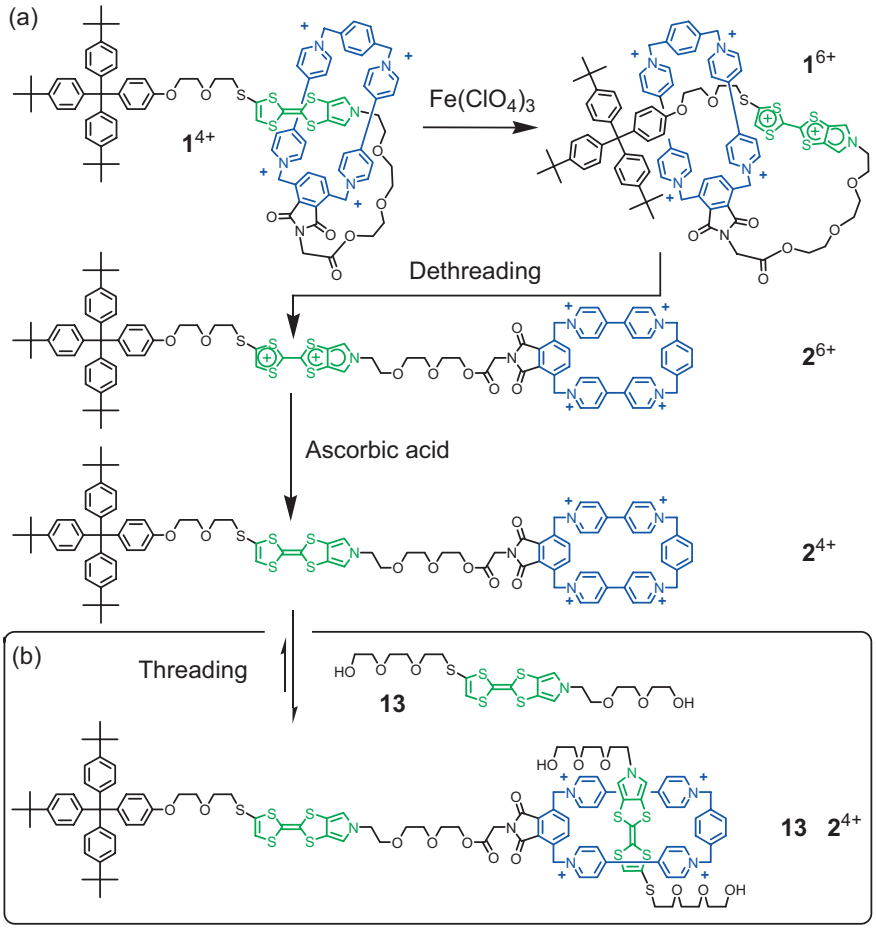

Scheme 3. a) Oxidation–reduction cycle of the interlocked compound 1^{4+} leading to the initial formation of the linear, doubly oxidized compound 2^{6+}, which is reduced with AA to form the neutral linear non-interlocked isomer 2^{4+}. b) Addition of the MPTTF thread **13** leads to formation of the [2]pseudoroaxane $\mathbf{13}\subset\mathbf{2}^{4+}$ thereby partially restoring the intensity of the CT band.

to bind another guest, that is, the Serpent's mouth is now open to bite onto another tail. To confirm that the linear form 2^{4+} is present, we selected a solution sample that offered a partial restoration of the CT band to 57 % of its original intensity, thereby defining a $1^{4+}/2^{4+}$ ratio of ≈57:43. When an excess of the MPTTF thread **13** is added to the solution (see Fig. S11) the CT band is restored up to 90 %.[35] This observation clearly indicates that the $CBPQT^{4+}$ cyclophane of the linear 2^{4+} is still present and intact within the solution and that it is capable of forming a [2]pseudorotaxane, $\mathbf{13}\subset\mathbf{2}^{4+}$, with the free threadlike MPTTF unit **13**. We excluded degradation based on the integrity of the 525 nm absorption band for 9000 s and longer (15 h). The rethreading experiment of 2^{4+} also supports the idea that the doubly oxidized 1^{6+} and 2^{6+} are not breaking apart into the free MPTTF and $CBPQT^{4+}$ fragments. If fragmentation had occurred, the resulting MPTTF moiety, represented as either a thread or a half-dumbbell, would form a [2]pseudorotaxane with the fragmented $CBPQT^{4+}$ ring. Quantitatively, the kinetics of the dethreading process was followed by probing the time-dependent decrease of the CT band located at 830 nm after each oxidation–reduction cycle, originating from the MPTTF unit encircled by $CBPQT^{4+}$ in any remaining 1^{4+} (Fig. 8). Assuming the operation of first order kinetics (see Supporting Information), a $\Delta G^{\ddagger}$ value of 22.8 kcal mol^{-1} at 293 K was obtained for the oxidation-induced dethreading process of 1^{6+} to form the linear doubly oxidized form 2^{6+}.

It is evident from the experimental results that the initially interlocked molecular ouroboros 1^{4+} can be converted into the non-interlocked linear form 2^{4+} by applying an oxidation–reduction cycle for an appropriate period of time. This behavior constitutes the newest and most recent example of how to harness the free energy of approximately 9 kcal mol^{-1} generated[12] by the Coulombic repulsion formed between the doubly oxidized $MPTTF^{2+}$ unit and the tetracationic ring component $CBPQT^{4+}$ to perform a task that would otherwise be significantly slower. Consequently, we estimate the barrier of $1^{4+}\rightarrow 2^{4+}$ to be ≈32 kcal mol^{-1} at 293 K. In this case 2^{4+} ends up looking like an image of the Serpent that has released its own tail.

2.9. Chemical Oxidation-Induced Dethreading Experiments Monitored by ^{1}H NMR Spectroscopy

In order to unambiguously confirm the formation of the linear form, the entire process was investigated by ^{1}H NMR spectroscopy. The spectra of 1^{4+} in

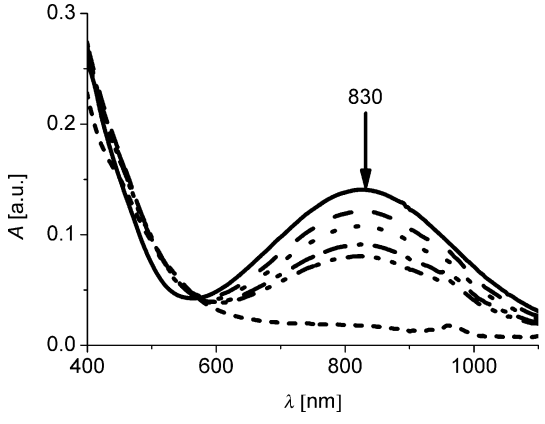

Figure 8. Overview of the decrease observed in the CT band, originating from remaining 1^{4+} in solution after subjecting the initial solution of 1^{4+} in MeCN to a chemical oxidation–reduction cycle. The initial solution of 1^{4+} (solid line) was oxidized for either 1800 s (dashed line), 3600 s (dotted line), 6200 s (dash-dotted line), 9000 s (dash-dot-dotted line), or 55 000 s (short-dashed line).

CD_3CN was recorded at 298 K before (Fig. 9a) and after oxidation by the addition of 2.0–2.5 equivalents of the chemical oxidant, tris(4-bromophenyl)ammoniumyl hexachloroantimonate ($TASbCl_6$), and at various times after the oxidation (Fig. 9b–f). The addition of the chemical oxidant to $\mathbf{1}^{4+}$ led to two major observations of the peak location and time dependant evolution of the spectrum. The very broad signals assigned to either the resonances of the bipyridinium H_α ($\delta = 8.8$–9.2 ppm) or H_β ($\delta = 8.1$–8.4 ppm) protons in the aromatic region of the unoxidized interlocked compound $\mathbf{1}^{4+}$ simplify into sets of distinct doublets after the compound has been maintained in the doubly oxidized $MPTTF^{2+}$ state for more than 39 min (Fig. 9e).[36] In the case of the H_β protons, a single doublet consisting of two overlapping doublets is seen at 8.20 ppm after 39 min, whereas the H_α protons are found as two distinct doublets resonating at 8.80 and 8.89 ppm, respectively. Moreover, the protons associated with the $MPTTF^{2+}$ unit, H_{TTF}, H_{Pyr}, and H_{SCH_2} protons all shifted downfield ($\delta = 8.96$, 8.10, and 3.60 ppm, respectively) relative to the position at which they are found in the linear dumbbell compound **11** ($\delta = 6.51$, 6.77, and 2.95 ppm, respectively). Previous investigations have shown that this behavior is entirely consistent[37] with the formation of an unencircled $MPTTF^{2+}$ dication and therefore of $\mathbf{2}^{6+}$.

Furthermore, the simplification of the ^{1}H NMR spectrum upon oxidation for more than 39 min is consistent with the formation of an uncomplexed species $\mathbf{2}^{6+}$, in which the bipyridinium units experience greater rotational freedom than in the initially interlocked compound, $\mathbf{1}^{4+}$, to give a degenerate signal. Subsequently, the addition of Zn dust reduces the $MPTTF^{2+}$ to its neutral form. The spectrum retains its high simplicity as opposed to the self-complex $\mathbf{1}^{4+}$, and thus unambiguously reveals the generation of the uncomplexed linear form $\mathbf{2}^{4+}$ after the oxidation–reduction cycle (Fig. 9g, for assignments see Fig. S14).

Secondly, it is evident from the time-lapsed ^{1}H NMR spectra that there is a dynamic evolution of the doubly oxidized compound. Directly after addition and mixing (≈1 min) of the chemical oxidant into the solution of $\mathbf{1}^{4+}$, a more complex spectrum is observed (Fig. 9b) as compared to the spectrum after 39 min (Fig. 9e). An indicative peak that represents this process very well is the dominant singlet at 7.85 ppm (Fig. 9b). The intensity of this peak rapidly decreases as a function of time (Fig. 9, marked by dashed boxes), until its disappearance after 39 min. Quite a few peaks are noted to suffer the same fate, suggesting that they represent the situation where the doubly oxidized $MPTTF^{2+}$ unit is still found in a self-complexed form, that is, $\mathbf{1}^{6+}$. Concomitant with these changes, there are observed peaks whose intensity increases over the same time frame, exemplified by the H_{TTF} signal from the doubly oxidized $MPTTF^{2+}$ unit observed at 8.96 ppm, thereby confirming the formation of $\mathbf{2}^{6+}$. Based on these assignments it is evident that the chemically induced dethreading process happens to take place faster under the conditions used for the ^{1}H NMR experiment ($TASbCl_6$), compared to those used in the UV-vis-NIR absorption experiment ($Fe(ClO_4)_3$).

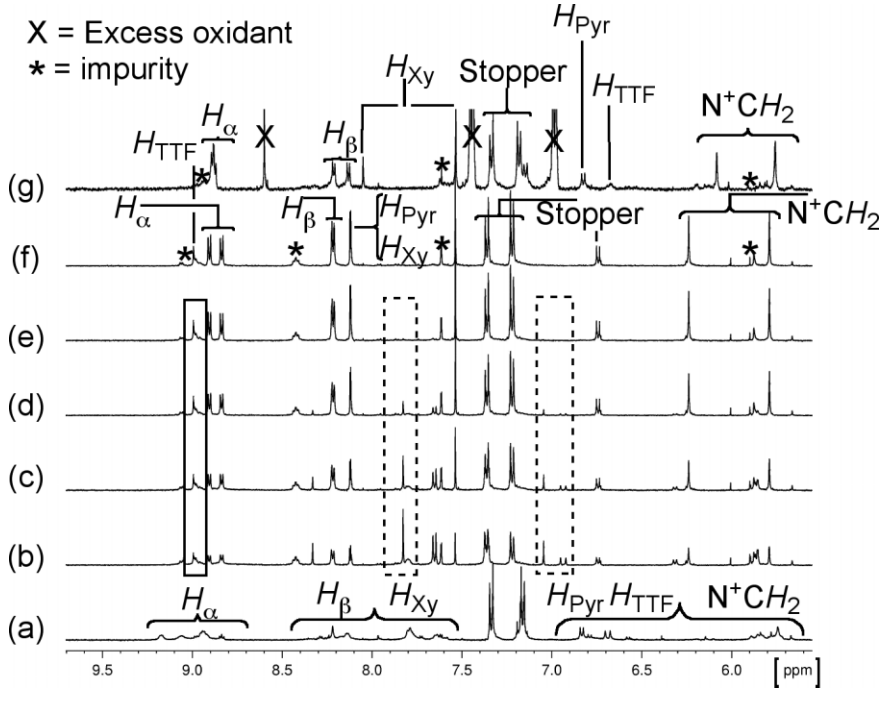

Figure 9. Downfield region of the ^{1}H NMR spectra (CD_3CN, 500 MHz) of $\mathbf{1}^{4+}$ at 298 K showing a) the spectrum of $\mathbf{1}^{4+}$ before oxidation and the evolution of the spectrum after the addition of 2.0–2.5 equiv of the oxidant at b) 1 min, c) 3 min, d) 13 min, e) 39 min, f) 360 min [38], and g) after reduction with Zn powder to generate the neutral, linear form $\mathbf{2}^{4+}$.

2.10. Springlike Properties of the Mechanically Interlocked Molecular Ouroboros

The analogy of a molecular ouroboros paints a straightforward picture of the structure that constitutes the interlocked molecule $\mathbf{1}^{4+}$. However, the structural analogy of the Serpent biting its own tail does not entirely represent the complex and dynamic properties of the interlocked molecule observed in the various solution studies. An analogy to a wound spring is more likely to represent the intrinsic functional qualities of the system. The springlike properties of $\mathbf{1}^{4+}$ emerge from a blend of the curved nature of the interlocked structure of the molecule with the Coulombic charge–charge repulsion. It is interesting to note that these qualities resemble the ones used to describe the pressure build up that occurs when nucleic acid is packaged into a virus capsid.[5b] The initially interlocked molecule $\mathbf{1}^{4+}$ both energetically and structurally resembles a spring in its initial state in the sense that it cannot perform a given task before energy

has been fed into the system. For a macroscopic spring this energy can be supplied by a mechanical winding motion, that is, torsion, or through a compression of the spring. In this molecular version, however, one can add energy to increase the tension in the already mechanically wound structure by providing either a chemical energy supply as either $Fe(ClO_4)_3$ or $TASbCl_6$ or by an electrical energy supply (CV). The resulting electrostatic energy mimics the tension buildup of a spring in the sense that the Coulombic repulsion between the $MPTTF^{2+}$ unit and the tetracationic cyclophane $CBPQT^{4+}$ creates a high energy state of the still interlocked molecule, that is, $\mathbf{1}^{6+}$. This high-energy conformation returns to the resting state of the self-complex once the electrostatic energy is removed by reduction. Unlike a conventional spring, however, the molecular ouroboros can be unwound in an irreversible way whereby it releases built-up tension worthy of ≈ 9 kcal mol^{-1} by overcoming an internal steric barrier to generate the linear and non-complexed structure, $\mathbf{2}^{6+}$. This unwinding process is both quantified from the UV-vis-NIR experiment and confirmed independently from ^{1}H NMR chemical-oxidation experiments. Just as macroscopic springs operate reversibly, the initially interlocked molecular ouroboros $\mathbf{1}^{4+}$ operates reversibly when tension is rapidly applied and removed, but performs like a single release spring[38] when it spends that tension force irreversibly to generate the linear form.

3. Conclusions

A mechanically interlocked molecule, $\mathbf{1}^{4+}$, in the form of a molecular ouroboros has been constructed and shown subsequently to display a number of dynamic properties in its interlocked ground state conformation, $\mathbf{1}^{4+}$, as well as in the doubly oxidized $\mathbf{1}^{6+}$ state. The ground state of the compound was found to exist as a mixture of two interlocked isomers differing only in the relative orientation of the MPTTF unit found inside the $CBPQT^{4+}$ ring component. The interconversion of the two isomers was followed by dynamic VT ^{1}H NMR spectroscopy and a barrier of 14 kcal mol^{-1} was found for the flipping motion of the MPTTF unit. It was further found that applying an appropriate stimuli (chemical or electrochemical oxidation) to create the doubly oxidized $MPTTF^{2+}$ unit initially generated an interlocked high-energy conformation $\mathbf{1}^{6+}$ that was observed to relax to the non-interlocked, linear, low-energy state $\mathbf{2}^{6+}$ in condition-specific time periods; ≈ 30 min for $TASbCl_6$ and ≈ 10 h for $Fe(ClO_4)_3$. Subsequently, addition of a suitable reduction agent (aqueous ascorbic acid or zinc powder) after the occurrence of the oxidation-induced rearrangement generates the linear state $\mathbf{2}^{4+}$ as determined by both UV-vis-NIR absorption and ^{1}H NMR spectroscopy. The dethreading process to form $\mathbf{2}^{4+}$ was followed in detail by UV-vis-NIR absorption spectroscopy which allowed the barrier of dethreading to be estimated to 22.8 kcal mol^{-1} at 293 K for the process that converts $\mathbf{1}^{6+}$ into $\mathbf{2}^{6+}$ using $Fe(ClO_4)_3$ as the oxidant. The emerging springlike qualities arise from the combination of the steric constraints imposed by the curved interlocked structure and electrostatic repulsion, and in this instance, represents an important stepping stone towards performing work on the molecular scale.

4. Experimental

General: All reactions were carried out in an atmosphere of anhydrous Argon. Solvents were dried according to literature procedures.[39] The high pressure experiment was carried out on a Psika high-pressure apparatus. All reagents used were standard grade and used as received from Aldrich or Fluka without further purification. Compounds **3**,[10b] **4**,[40] **7**,[41] **10**,[8b] **12**·2 PF_6,[9a] and **13**[42] were all prepared according to literature procedures. Analytical thin-layer chromatography (TLC) was carried out on Merck DC-alufolien Kiselgel 60 F_{254} 0.2 mm thickness precoated TLC plates. The plates were inspected under UV light and in some cases developed using iodine vapor. Column chromatography was carried out by using silica gel 60F (Merck, 9385, 0.040–0.063 mm) whereas preparative thin layer chromatography (PTLC) was carried out on Merck precoated PTLC plates. Deactivated silica was prepared by adding 2 % triethylamine ($(Et)_3N$) to a slurry of silica gel in CH_2Cl_2 followed by removal of the organic solvent by filtration. The deactivated silica was resuspended in fresh CH_2Cl_2 and the solvent removed before use. Melting points were determined on an Büchi melting point apparatus and are uncorrected. ^{1}H NMR spectra were recorded on a Varian Gemini (300 MHz), a Varian Inova (500 MHz), or on a Bruker Avance (500 MHz) at room temperature. Residual solvent peaks were used as an internal standard. Low-resolution ESI spectra were obtained with a Finnigan MAT SSQ710 triple quadropole instrument. High resolution MALDI and ESI spectra were collected with a Fourier transform–ion cyclotron resonance mass spectrometer (FT-ICR MS) instrument. UV-vis-NIR spectra were recorded on a Shimadzu UV-160 instrument or on a Cary Bio 100 instrument. Electrochemical investigations were performed on a Princeton Applied Research Potentiostat/Galvanostat Model 263 A. Elemental analyses were performed by Atlantic Microlab, Inc.

*Compound **6***: The MPTTF compound **3** (200 mg, 0.41 mmol) and the stopper **4** (305 mg, 0.44 mmol) were dissolved in anhydrous THF (15 mL) and degassed (Ar, 15 min). A solution of $CsOH{\cdot}H_2O$ (75 mg, 0.43 mmol) in anhydrous MeOH (3 mL) was added dropwise using a syringe. The reaction mixture was stirred for 16 h causing the initial clear yellow solution to become light green and cloudy. The solvent was then removed in vacuo to yield a yellow solid that was redissolved in CH_2Cl_2 (100 mL) washed with H_2O (3×100 mL) and dried ($MgSO_4$). Column chromatography (SiO_2, eluent: cyclohexane/CH_2Cl_2, 1:1 v/v) of the resulting yellow solid gave two broad yellow bands containing the tosylated product **5** and the detosylated product **6**, respectively. The two fractions were combined and concentrated in vacuo to provide a yellow compound (275 mg) containing the mixture of **5** and **6**, which was dissolved in anhydrous THF:MeOH (1:1 v/v, 100 mL) and thoroughly degassed (Ar, 15 min). Sodium methoxide (NaOMe; 332 mg, 6.15 mmol) was added in one portion, whereupon the reaction mixture was refluxed for 1 h. The solvent was removed in vacuo and the yellow residue was dissolved in CH_2Cl_2 (100 mL), washed with H_2O (2×100 mL), and dried ($MgSO_4$). Removal of the solvent in vacuo gave a yellow oil that was purified by column chromatography (SiO_2, eluent: cyclohexane/CH_2Cl_2 1:1 v/v). The yellow band ($R_f = 0.15$) was collected and the solvent evaporated to give the title compound **6** (186 mg, 53 %) as a yellow oil. ^{1}H NMR (300 MHz, $CDCl_3$): $\delta = 1.30$ (s, 27 H), 2.95 (t, $J = 6.5$ Hz, 2 H), 3.75 (t, $J = 6.5$ Hz, 2 H), 3.82 (t, $J = 6.5$ Hz, 2 H), 4.08 (t, $J = 6.5$ Hz, 2 H), 6.53 (d, $J = 2.7$ Hz, 2 H), 6.75 (d, $J = 8.7$ Hz, 2 H), 7.02 (s, 1 H), 7.07–7.09 (m, 8 H), 7.21–7.25 (m, 6 H), 8.06 (s, 1 H); MS (MALDI): *m/z* (%): 872 (5) [M^+ + Na], 849 (100) [M^+]; HiRes-FT-MALDI-MS: *m/z* calcd for $C_{49}H_{55}NO_2S_5^+$: 849.2831; found: 849.2851; elemental analysis calcd (%) for $C_{49}H_{55}NO_2S_5$: C 69.21, H 6.52, N 1.65, S 18.86; found: C 69.11, H 6.52, N 1.75, S 18.63.

*Compound **8***: The MPTTF derivative **6** (530 mg, 0.62 mmol), the iodo TEG derivative **7** (230 mg, 0.68 mmol), and hexane washed NaH (74 mg, 3.1 mmol) were dissolved in anhydrous DMF (30 mL). The

yellow reaction mixture was stirred for 3 h at room temperature. The solvent was removed under reduced pressure to yield a brown oil, which was subsequently redissolved in CH_2Cl_2. The organic phase was washed with H_2O (2 × 100 mL) and dried ($MgSO_4$) before the solvent was removed in vacuo. The resulting residue was purified by column chromatography (SiO_2, eluent: CH_2Cl_2/EtOAc 9:1 v/v) and the broad yellow band ($R_f = 0.4$) was collected and concentrated to provide the title compound **8** (535 mg, 81 %) as a yellow semi-crystalline solid. ^{1}H NMR (300 MHz, $CDCl_3$): δ = 1.30 (s, 27 H), 1.68–1.85 (m, 6 H), 2.95 (t, *J* = 6.5 Hz, 2 H), 3.57–3.84 (m, 18 H), 4.09 (t, *J* = 6.5 Hz, 2 H), 4.63 (s, 1 H), 6.51 (s, 2 H), 6.77 (d, *J* = 8.7 Hz, 2 H), 7.06–7.09 (m, 9 H), 7.21–7.25 (m, 6 H); MS(MALDI): *m/z* (%): 1088 (5) [M^+ + Na], 1065 (100) [M^+]; HiRes-FT-MALDI-MS: *m/z* calcd for $C_{60}H_{75}NO_6S_5^+$: 1065.4192; found: 1065.4142.

Compound ***9***: The THP-protected alcohol **8** (530 mg, 0.50 mmol) was dissolved in anhydrous THF/EtOH (40 mL 1:1 v/v) and degassed (Ar, 15 min). A catalytic amount of *para*-toluene sulfonic acid (PTSA) was added to the yellow solution, which resulted in a color change to green. The reaction mixture was stirred for 4 h at room temperature. The reaction was quenched by addition of CH_2Cl_2 (100 mL), and washing with a saturated aqueous solution of $NaHCO_3$ (100 mL) and H_2O (100 mL). The organic phase was dried ($MgSO_4$) and the solvent was removed in vacuo, whereupon the residue was purified by column chromatography (deactivated SiO_2, eluent: CH_2Cl_2/EtOAc 9:1 v/v). The broad yellow band ($R_f = 0.3$) was collected and the solvent evaporated to afford the title compound **9** (250 mg, 51 %) as a yellow semi-solid. ^{1}H NMR (300 MHz, $CDCl_3$): δ = 1.31 (s, 27 H), 2.09 (s, 1 H), 2.96 (t, *J* = 6.5 Hz, 2 H), 3.55–3.84 (m, 14 H), 3.98 (t, *J* = 6.5 Hz, 2 H), 4.10 (t, *J* = 6.5 Hz, 2 H), 6.50 (s, 2 H), 6.78 (d, *J* = 8.7 Hz, 2 H), 7.06–7.09 (m, 9 H), 7.21–7.27 (m, 6 H); MS (MALDI): *m/z* (%): 1004 (20) [M^+ + Na], 981 (100) [M^+]; HiRes-FT-MALDI-MS: *m/z* calcd for $C_{55}H_{67}NO_5S_5^+$: 981.3617; found: 981.3641.

Half-Dumbbell Compound ***11***: The MPTTF unit **9** (250 mg, 0.25 mmol) and the dibromide **10** (109 mg, 0.27 mmol) were dissolved in CH_2Cl_2 (20 mL). DCC (105 mg, 0.50 mmol) and 4-(*N*,*N*-dimethylamino)-pyridine (DMAP) (catalytic amount) were added and the yellow reaction mixture was stirred for 3 h at room temperature. The solvent was removed, yielding a reddish solid which was purified by column chromatography (SiO_2, eluent: cyclohexane/EtOAc 7:3 v/v). The broad yellow band ($R_f = 0.5$) was collected and the solvent removed yielding the title compound **11** (335 mg, 94 %) as a yellow semi-solid contaminated with traces of DCC byproducts [43]. ^{1}H NMR (300 MHz, $CDCl_3$): δ = 1.30 (s, 27 H), 2.95 (t, *J* = 6.5 Hz, 2 H), 3.59–3.78 (m, 12 H), 3.80–3.84 (m, 2 H), 4.09 (t, *J* = 6.5 Hz, 2 H), 4.33–4.37 (m, 2 H), 4.44 (s, 2 H), 4.93 (s, 4 H), 6.51 (s, 1 H), 6.77 (d, *J* = 8.7 Hz, 2 H), 7.06–7.08 (m, 10 H), 7.21–7.24 (m, 6 H), 7.70 (s, 2 H); HiRes-FT-MALDI-MS: *m/z* calcd for $C_{67}H_{74}Br_2N_2O_8S_5^+$: 1354.2388; found 1354.2395.

Self-complex ***1***·4 PF_6: A solution of the dumbbell compound **11** (335 mg, 0.25 mmol) and **12**·2 PF_6 (278 mg, 0.39 mmol) in anhydrous DMF (10 mL) was transferred to a Teflon tube and subjected to 10 kbar pressure at room temperature for 4 d. The resulting intense green solution was directly subjected to column chromatography (SiO_2). Unreacted dumbbell **11** was eluted with Me_2CO, whereupon the eluent was changed to Me_2CO/NH_4PF_6 (100:1 v/w) and the green band was collected. Most of the solvent was removed in vacuo, followed by addition of H_2O (25 mL). The resulting green precipitate was collected by filtration, washed with H_2O (100 mL) and Et_2O (50 mL) providing 150 mg (27 %) of a green solid shown to consist of a mixture[19] of the self-complexed [2]rotaxane **1**·4 PF_6 and the noncomplexed, linear cyclophane **2**·4 PF_6. The self-complexed cyclophane **1**·4 PF_6 was separated by preparative thin-layer chromatography of small batches (15 mg) of the original mixture using Me_2CO/NH_4PF_6 (100:1 v/w) as the eluent providing the pure **1**·4 PF_6 (7–8 mg, 50 %) as a green solid. mp > 215–225 °C (decomposed without melting). Data for **1**·4 PF_6: ^{1}H NMR (CD_3COCD_3, 500 MHz, 198 K) δ = 1.22 (s, 27 H), 3.06 (bs, 1.2 H), 3.22 (bs, 0.8 H), 3.70–3.75 (m, 6 H), 3.87 (bs, 4 H), 4.02 (bs, 2 H), 4.21–4.25 (m, 4 H), 4.67 (bs, 2 H), 4.76–4.78 (m, 2 H), 5.65 (s, 0.4 H), 5.72 (s, 0.6 H), 6.06–6.27 (m, 4 H), 6.79–6.95 (m 6 H), 7.05–7.20 (m, 10 H), 7.33–7.36 (m, 6 H), 7.90 (s, 0.8 H), 7.99 (s, 1.2 H), 8.14 (s, 0.8 H), 8.19 (s, 1.2 H), 8.41–8.47 (m, 3 H), 8.60–8.65 (m, 3 H), 8.79–8.89 (m, 4 H), 9.17 (d, *J* = 6.0 Hz; 2 H), 9.57–9.82 (m, 6 H); MS(ESI): *m/z* (%): 402.7 (30) [$M - 4PF_6$]$^{4+}$, 585.2 (30) [$M - 3PF_6$]$^{3+}$, 950.4 (100) [$M - 2PF_6$]$^{2+}$; elemental analysis calcd (%) for $C_{95}H_{98}F_{24}N_6O_8P_4S_5 \cdot H_2O$: C 51.63, H 4.56, N 3.80, S 7.25; found: C 51.49, H 4.94, N 4.01, S 6.89.

Data for **2**$^{6+}$: (Oxidation [44] of **1**·4 PF_6): ^{1}H NMR (CD_3CN, 298 K, purple): δ = 1.26 (s, 27 H), 3.59–3.64 (m, 8 H), 3.84–3.86 (m, 2 H), 3.90 (t, *J* = 5.5 Hz, 2 H), 4.01–4.05 (m, 4 H), 4.27 (t, *J* = 5.5 Hz, 2 H), 4.39 (s, 2 H), 4.56 (t, *J* = 5.5 Hz, 2 H), 5.76 (s, 4 H), 6.21 (s, 4 H), 6.71 (d, *J* = 9.0 Hz), (7.18–7.20 (m, 8 H), 7.32–7.34 (m, 6 H), 7.51 (s, 4 H), 8.08 (s, 2 H), 8.10 (s, 2 H), 8.19 (d, *J* = 7.0 Hz, 8 H), 8.80 (d, *J* = 7.0 Hz, 4 H), 8.80 (d, *J* = 7.0 Hz, 4 H), 8.96 (s, 1 H).

Data for **2**$^{4+}$: ^{1}H NMR (CD_3CN, 298 K, yellow): δ = 1.28 (s, 27 H), 2.99 (t, *J* = 6.0 Hz, 2 H), 3.53–3.77 (m, 14 H), 4.06–4.08 (m, 4 H), 4.32 (s, 2 H), 5.73 (s, 4 H), 6.05 (s, 4 H), 6.64 (bs, 1 H), 6.80 (d, *J* = 8.5 Hz, 2 H), 7.11–7.16 (m, 10 H), 7.30–7.32 (m, 6 H), 7.50 (s, 4 H), 8.02 (s, 2 H), 8.10 (d, *J* = 7.0 Hz, 4 H), 8.18 (d, *J* = 7.0 Hz, 4 H), 8.83–8.86 (m, 8 H).

Received: October 1, 2006
Revised: December 22, 2006

[1] a) V. Balzani, A. Credi, M. Venturi, *Molecular Devices and Machines: A Journey into the Nano World*, Wiley-VCH, Weinheim, Germany **2003**. b) G. S. Kottas, L. I. Clarke, D. Horinek, J. Michl, *Chem. Rev.* **2005**, *105*, 1281. c) N. N. P. Moonen, A. H. Flood, J. M. Fernandez, J. F. Stoddart, *Top. Curr. Chem.* **2005**, *262*, 99. d) A. B. Braunschweig, B. H. Northrop, J. F. Stoddart, *J. Mater. Chem.* **2006**, *16*, 32. e) S. Bonnet, J. P. Collin, M. Koizumi, P. Mobian, J.-P. Sauvage, *Adv. Mater.* **2006**, *18*, 1239. f) T. A. V. Khuong, J. E. Nunez, C. E. Godinez, M. A. Garcia-Garibay, *Acc. Chem. Res.* **2006**, *39*, 413. g) Y. Shirai, A. J. Osgood, Y. M. Zhao, Y. X. Yao, L. Saudan, H. B. Yang, Y. H. Chiu, L. B. Alemany, T. Sasaki, J. F. Morin, J. M. Guerrero, K. F. Kelly, J. M. Tour, *J. Am. Chem. Soc.* **2006**, *128*, 4854. h) S. Hiraoka, T. Tanaka, M. Shionoya, *J. Am. Chem. Soc.* **2006**, *128*, 13 038.

[2] a) R. K. Soong, G. D. Bachand, H. P. Neves, A. G. Olkhovets, H. G. Craighead, C. D. Montemagno, *Science* **2000**, *290*, 1555. b) M. Schliwa, G. Woehlke, *Nature* **2003**, *422*, 759. c) A. Yildiz, M. Tomishige, R. D. Vale, P. R. Selvin, *Science* **2004**, *303*, 676. d) W. B. Sherman, N. C. Seeman, *Nano Lett.* **2004**, *4*, 1203. e) J. V. Hernandez, E. R. Kay, D. A. Leigh, *Science* **2004**, *306*, 1532. f) Y. Tian, Y. He, Y. Chen, P. Yin, C. D. Mao, *Angew. Chem. Int. Ed.* **2005**, *44*, 4355. g) J. Bath, S. J. Green, A. J. Turberfield, *Angew. Chem. Int. Ed.* **2005**, *44*, 4358. h) M. N. Chatterjee, E. R. Kay, D. A. Leigh, *J. Am. Chem. Soc.* **2006**, *128*, 4058. i) V. Balzani, M. Clemente-Leon, A. Credi, B. Ferrer, M. Venturi, A. H. Flood, J. F. Stoddart, *Proc. Natl. Acad. Sci. USA* **2006**, *103*, 1178. j) R. Eelkema, M. M. Pollard, J. Vicario, N. Katsonis, B. S. Ramon, C. W. M. Bastiaansen, D. J. Broer, B. L. Feringa, *Nature* **2006**, *440*, 163.

[3] a) H. Hess, G. D. Bachand, V. Vogel, *Chem. Eur. J.* **2004**, *10*, 2110. b) G. D. Bachand, S. B. Rivera, A. Carroll-Portillo, H. Hess, M. Bachand, *Small* **2006**, *2*, 381. c) M. G. L. van den Heuvel, M. P. De Graaff, C. Dekker, *Science* **2006**, *312*, 910. d) C. Z. Dinu, J. Opitz, W. Pompe, J. Howard, M. Mertig, S. Diez, *Small* **2006**, *2*, 1090.

[4] a) M. D. Wang, M. J. Schnitzer, H. Yin, R. Landick, J. Gelles, S. M. Block, *Science* **1998**, *282*, 902. b) R. D. Vale, R. A. Milligan, *Science* **2000**, *288*, 88. c) D. E. Smith, S. J. Tans, S. B. Smith, S. Grimes, D. L. Anderson, C. Bustamante, *Nature* **2001**, *413*, 748. d) A. Evilevitch, L. Lavelle, C. M. Knobler, E. Raspaud, W. M. Gelbart, *Proc. Natl. Acad. Sci. USA* **2003**, *100*, 9292.

[5] a) R. D. Astumian, P. Hanggi, *Phys. Today* **2002**, *55*, 33. b) S. Tzlil, J. T. Kindt, W. M. Gelbart, A. Ben-Shaul, *Biophys. J.* **2003**, *84*, 1616. c) G. Oster, H. Y. Wang, *Trends Cell Biol.* **2003**, *13*, 114. d) M. Downton, M. Plischke, M. J. Zuckermann, D. Phil, E. Craig, H. Linke, *Biophys. J.* **2005**, *88*, 506 A.

[6] For details on the various uses of [2]catenanes refer to: a) M. Asakawa, P. R. Ashton, V. Balzani, A. Credi, C. Hamers, G. Mattersteig,

M. Montalti, A. N. Shipway, N. Spencer, J. F. Stoddart, M. S. Tolley, M. Venturi. A. J. P. White, D. J. Williams, *Angew. Chem. Int. Ed.* **1998**, *37*, 333. b) P. Mobian, J.-M. Kern, J.-P. Sauvage, *Angew. Chem. Int. Ed.* **2004**, *43*, 4392. c) C. P. Collier, G. Mattersteig, E. W. Wong, Y. Liu, K. Beverly, J. Sampio, F. M. Raymo, J. F. Stoddart, J. R. Heath, *Science* **2000**, *289*, 1172. d) D. W. Steuerman, H.-R. Tseng, A. J. Peters, A. H. Flood, J. O. Jeppesen, K. A. Nielsen, J. F. Stoddart, J. R. Heath, *Angew. Chem. Int. Ed.* **2004**, *43*, 6486. e) J. V. Hernandez, E. R. Kay, D. A. Leigh, *Science* **2004**, *306*, 1532.

[7] A more detailed description of the various types of [2]rotaxanes and their uses can be found in: a) G. Schill, *Catenanes, Rotaxanes and Knots*, Academic, New York **1971**. b) D. B. Amabilino, J. F. Stoddart, *Chem. Rev.* **1995**, *95*, 2725. c) F. Vögtle, T. Dunnwald, T. Schmidt, *Acc. Chem. Res.* **1996**, *29*, 451. d) G. A. Breault, C. A. Hunter, P. C. Mayers, *Tetrahedron* **1999**, *55*, 5265. e) T. J. Hubin, A. G. Kolchinski, A. L. Vance, D. H. Busch, *Adv. Supramol. Chem.* **1999**, *6*, 237. f) *Molecular Catenanes, Rotaxanes and Knots* (Eds: J.-P. Sauvage, C. Dietrich-Buchecker), VCH-Wiley, Weinheim, Germany **1999**. g) L. Raehm, D. G. Hamilton, J. K. M. Sanders, *Synlett* **2002**, 1743. h) J. F. Stoddart, H.-R. Tseng, *Proc. Natl. Acad. Sci. USA* **2002**, *99*, 4797. i) G. Gatti, S. León, J. K. Y. Wong, G. Bottari, A. Altieri, M. A. F. Morales, S. J. Teat, C. Frochot, D. A. Leigh, A. M. Brouwer, F. Zerbetto, *Proc. Natl. Acad. Sci. USA* **2003**, *100*, 10. j) D. A. Leigh, E. M. Pérez, *Chem. Commun.* **2004**, 2262. k) J.-P. Sauvage, *Chem. Commun.* **2005**, 1507. l) D. S. Marlin, C. Gonzalez, D. A. Leigh, A. M. Z. Slawin, *Angew. Chem. Int. Ed.* **2006**, *45*, 77.

[8] The construction of a molecular elevator has been described, see: a) J. D. Badjic, V. Balzani, A. Credi, S. Silvi, J. F. Stoddart, *Science* **2004**, *303*, 1845. As well as configurable and reconfigurable molecular switches, see: b) Y. Liu, S. Saha, S. A. Vignon, A. H. Flood, J. F. Stoddart, *Synthesis* **2005**, *19*, 3437.

[9] a) P.-L. Anelli, P. R. Ashton, R. Ballardini, V. Balzani, M. Delgado, M. T. Gandolfi, T. T. Goodnow, A. E. Kaifer, D. Philp, M. Pietraszkiewicz, L. Prodi, M. V. Reddington, A. M. Z. Slawin, N. Spencer, J. F. Stoddart, C. Vicent, D. J. Williams, *J. Am. Chem. Soc.* **1992**, *114*, 193. b) M. Asakawa, W. Dehaen, G. L'abbé, S. Menzer, J. Nouwen, F. M. Raymo, J. F. Stoddart, D. J. Williams, *J. Org. Chem.* **1996**, *61*, 9591.

[10] A wide array of [2]pseudorotaxanes formed by the inclusion of either NP- or (MP)TTF-derivatives in the cavity of $CBPQT^{4+}$ have been reported in the literature. The trend is always that the stronger π-electron donor (MP)TTF is much more strongly bound in the cavity of the tetracationic cyclophane compared with NP, a much weaker π-electron donor. A K_a value of $768\,M^{-1}$ has been reported for the [2]pseudorotaxane formation in CH_3CN between 1,5-dihydroxynaphthalene and $CBPQT^{4+}$ at room temperature. See, a) R. Castro, K. R. Nixon, J. D. Evenseck, A. E. Kaifer, *J. Org. Chem.* **1996**, *61*, 7298. A comparable unsubstituted MPTTF derivative has been reported to have a K_a value of $3900\,M^{-1}$ in Me_2CO at room temperature, see: b) J. O. Jeppesen, S. Nygaard, S. A. Vignon, J. F. Stoddart, *Eur. J. Org. Chem.* **2005**, 196.

[11] For reviews on TTF chemistry and other applications of this important building block, see: a) M. R. Bryce, *J. Mater. Chem.* **2000**, *10*, 589. b) M. B. Nielsen, C. Lomholt, J. Becher, *Chem. Soc. Rev.* **2000**, *29*, 153. c) J. L. Segura, N. Martín, *Angew. Chem. Int. Ed.* **2001**, *40*, 1372. d) G. Schukat, E. Fanghänel, *Sulfur Rep.* **2003**, *24*, 1. e) T. Otsubo, K. Takimiya, *Bull. Chem. Soc. Jpn.* **2004**, *77*, 43. f) J. O. Jeppesen, M. B. Nielsen, J. Becher, *Chem. Rev.* **2004**, *104*, 5115. g) A. Gorgues, P. Hudhomme, M. Sallé, *Chem. Rev.* **2004**, *104*, 5151. h) P. Frère, P. J. Skabara, *Chem. Soc. Rev.* **2005**, *34*, 69.

[12] a) S. Nygaard, B. W. Laursen, A. H. Flood, C. N. Hansen, J. O. Jeppesen, J. F. Stoddart, *Chem. Commun.* **2006**, 144. b) A. H. Flood, B. W. Laursen, S. Nygaard, J. O. Jeppesen, J. F. Stoddart, *Org. Lett.* **2006**, *8*, 2205.

[13] a) J. O. Jeppesen, K. Takimiya, F. Jensen, J. Becher, *Org. Lett.* **1999**, *1*, 1291. b) J. O. Jeppesen, K. Takimiya, F. Jensen, T. Brimert, K. Nielsen, N. Thorup, J. Becher, *J. Org. Chem.* **2000**, *65*, 5794.

[14] B. Brough, B. H. Northrop, J. J. Schmidt, H.-R. Tseng, K. N. Houk, J. F. Stoddart, C.-H. Ming, *Proc. Natl. Acad. Sci. USA* **2006**, *103*, 8583.

[15] Y. Liu, A. H. Flood, P. A. Bonvallet, S. A. Vignon, B. H. Northrop, H.-R. Tseng, J. O. Jeppesen, T. J. Huang, B. Brough, M. Baller, S. Magonov, S. D. Solares, W. A. Goddard, C.-M. Ho, J. F. Stoddart, *J. Am. Chem. Soc.* **2005**, *127*, 9745.

[16] a) S. Shinkai, M. Ishihara, K. Ueda, O. Manabe, *J. Chem. Soc. Perkin Trans. 2* **1985**, 511. b) P. Pallavicini, A. Perotti, B. Seghi, L. Fabbrizzi, *J. Am. Chem. Soc.* **1987**, *109*, 5139. c) A. Ueno, I. Suzuki, T. Osa, *J. Am. Chem. Soc.* **1989**, *111*, 6391. d) A. Ueno, I. Suzuki, M. Fukushima, M. Okhubo, T. Osa, F. Hamada, K. Murai, *Chem. Lett.* **1990**, 605. e) S. Minato, T. Osa, A. Ueno, *J. Chem. Soc., Chem. Commun.* **1991**, 107. f) I. K. Lednev, M. V. Alfimov, *Supramol. Sci.* **1994**, *1*, 55. g) M. Nakamura, A. Ikeda, N. Ise, T. Ikeda, H. Ikeda, F. Toda, A. Ueno, *J. Chem. Soc., Chem. Commun.* **1995**, 721. h) R. Corradini, A. Dossena, R. Marchelli, A. Panagia, G. Sartor, M. Saviago, A. Lombardi, V. Pavone, *Chem. Eur. J.* **1996**, *2*, 373. i) L. Fabbrizzi, M. Licchelli, P. Pallavicini, L. Parodi, *Angew. Chem.* **1998**, *110*, 838. j) L. Fabbrizzi, F. Foti, M. Licchelli, P. M. Maccarini, D. Sacchi, M. Zema, *Chem. Eur. J.* **2002**, *8*, 4965. k) Y. Takenaka, M. Higashi, N. Yoshida, *J. Chem. Soc. Perkin Trans. 2* **2002**, 615. l) Y. Inoue, M. Miyauchi, H. Nakajima, Y. Takashima, H. Yamaguchi, A. Harada, *J. Am. Chem. Soc.* **2006**, *128*, 8994. m) G. Cooke, P. Woisel, M. Bria, F. Delattre, J. F. Garety, S. Hewage, S. Gunatilaka, G. Rabani, G. M. Rosair, *Org. Lett.* **2006**, *8*, 1423.

[17] a) J. O. Jeppesen, J. Perkins, J. Becher, J. F. Stoddart, *Angew. Chem. Int. Ed.* **2001**, *40*, 1216. b) J. O. Jeppesen, K. A. Nielsen, J. Perkins, S. A. Vignon, A. Di Fabio, R. Ballardini, M. T. Gandolfi, M. Venturi, V. Balzani, J. Becher, J. F. Stoddart, *Chem. Eur. J.* **2003**, *9*, 2982. c) H.-R. Tseng, S. A. Vignon, P. C. Celestre, J. Perkins, J. O. Jeppesen, A. Di Fabio, R. Ballardini, M. T. Gandolfi, M. Venturi, V. Balzani, J. F. Stoddart, *Chem. Eur. J.* **2004**, *10*, 155. d) B. W. Laursen, S. Nygaard, J. O. Jeppesen, J. F. Stoddart, *Org. Lett.* **2004**, *6*, 4167. e) J. W. Choi, A. H. Flood, D. W. Steuerman, S. Nygaard, A. B. Braunscheig, N. N. P. Moonen, B. W. Laursen, Y. Luo, E. DeIonno, A. J. Peters, J. O. Jeppesen, K. Xu, J. F. Stoddart, J. R. Heath, *Chem. Eur. J.* **2006**, *12*, 261.

[18] F.-G. Klärner, F. Wurche, *J. Prakt. Chem.* **2000**, *7*, 609.

[19] The amount of the linear form $\mathbf{2}\cdot 4\,PF_6$ in the originally isolated solid containing $\mathbf{1}\cdot 4\,PF_6$ and $\mathbf{2}\cdot 4\,PF_6$ is estimated to be less than 10% by ^1H NMR spectroscopy.

[20] Some proportion of the compound is always lost using the PTLC purification method on account of the binder in the silica and the subsequent strong binding of the interlocked compound to the silica matrix, making it rather difficult to extract it after separation.

[21] a) M. P. L. Werts, M. van den Boogaard, G. M. Tsivgoulis, G. Hadziioannou, *Macromolecules* **2003**, *36*, 7004. b) S. J. Rowan, J. F. Stoddart, *Polym. Adv. Technol.* **2003**, *14*, 777. c) Y. Liu, P. A. Bonvallet, S. A. Vignon, S. I. Kahn, J. F. Stoddart, *Angew. Chem. Int. Ed.* **2005**, *44*, 3050.

[22] This assignment is consistent with what has been reported for a similar type of compound, see: a) Y. Liu, A. H. Flood, R. M. Moskowitz, J. F. Stoddart, *Chem. Eur. J.* **2005**, *11*, 369. b) Y. Liu, A. H. Flood, J. F. Stoddart, *J. Am. Chem. Soc.* **2004**, *126*, 9150.

[23] J. O. Jeppesen, J. Becher, *Eur. J. Org. Chem.* **2003**, *17*, 3245.

[24] R. K. Harris, *Nuclear Magnetic Resonance Spectroscopy*, Pitman, Marshfield, MA **1983**.

[25] a) J. O. Jeppesen, J. Becher, J. F. Stoddart, *Org. Lett.* **2002**, *4*, 557. b) J. O. Jeppesen, S. A. Vignon, J. F. Stoddart, *Chem. Eur. J.* **2003**, *9*, 4611.

[26] This observation has not been seen before by us or others for other mechanically interlocked molecules reported in references 10b, 13, 15, and 17.

[27] There is a small (<5%) amount of the unencircled MPTTF unit at +430 mV, presumably arising from either a trace contamination by $\mathbf{2}^{4+}$ or a minor translational isomer.

[28] The integrated area under the DPV peaks in the oxidative region (+0.3 to +0.9 V) is 80% of the area under the split reduction peak at

–0.2 V. This 20 % discrepancy was reproducible based on a DPV analysis of the as-prepared sample of the nanovalve, which contains the linear form as a ~ 10 % impurity prior to PTLC purification, see ref. [19]. This difference is ascribed to kinetic differences associated either with the encapsulated MPTTF unit or the diffusion of the oxidized $\mathbf{1}^{6+/5+/4+}$ versus the reduced $\mathbf{1}^{4+/3+/2+}$ redox states.

[29] The splitting has been ascribed to both chemical and electrochemical inequivalence of the bipyridinium units and, to date, no conclusive studies have verified the extent of each contribution. See refs. [6a] and [12b].

[30] a) V. Balzani, A. Credi, G. Mattersteig, O. A. Matthews, F. M. Raymo, J. F. Stoddart, M. Venturi, A. J. P. White, D. J. Williams, *J. Org. Chem.* **2000**, *65*, 1924. b) T. Yamamoto, H.-R. Tseng, J. F. Stoddart, V. Balzani, A. Credi, F. Marchioni, M. Venturi, *Collect. Czech. Chem. Commun.* **2003**, *68*, 1488.

[31] a) A. H. Flood, A. J. Peters, S. A. Vignon, D. W. Steuerman, H.-R. Tseng, S. Kang, J. R. Heath, J. F. Stoddart, *Chem. Eur. J.* **2004**, *10*, 6558. b) H.-R. Tseng, D. Wu, N. Fang, X. Zhang, J. F. Stoddart, *ChemPhysChem* **2004**, *5*, 111.

[32] T. J. Huang, A. H. Flood, B. Brough, Y. Liu, P. A. Bonvallet, S. S. Kang, C. W. Chu, T. F. Guo, W. X. Lu, Y. Yang, J. F. Stoddart, C. M. Ho, *IEEE Trans. Autom. Sci. Eng.* **2006**, *3*, 254.

[33] The originally isolated solid from the high-pressure reaction was used without PTLC purification in the chemical oxidation–reduction experiments followed either by UV-vis-NIR or ^{1}H NMR spectroscopic investigations. The small amount of the linear form, $\mathbf{2}^{4+}$, present in the sample prior to the oxidation–reduction cycle, allowed us to use the signals from $\mathbf{2}^{4+}$ as an internal reference in the ^{1}H NMR spectroscopy experiment.

[34] One could also envision that the oxidation-induced dethreading process would take place by twisting the $CBPQT^{4+}$ ring over the bulky, hydrophobic tetraarylmethane stopper at the end of the molecule, but the steric bulk of this part of the molecule, as probed by CPK modelling, leads us to assume that this barrier is much larger than the barrier imposed by the two diimide oxygens.

[35] The observed loss in CT-band intensity can either be attributed to a small amount of chemical degradation of the starting compound, but it has to be taken into account that the intensity of the CT band formed by a free MPTTF unit and the $CBPQT^{4+}$ cyclophane always will be weaker than in a real interlocked compound, on account of the equilibrium existing between the complexed and uncomplexed species.

[36] A set of peaks that are not assignable are seen at low intensity in the ^{1}H NMR spectrum after the initial oxidation of $\mathbf{1}^{4+}$. The peaks in question are marked with * in Figure 9f, as well as in Figure 9g. These peaks are thought to represent the oxidation of a MPTTF-containing byproduct or degradation product.

[37] S. A .Vignon, J. F. Stoddart, *Collect. Czech. Chem. Commun.* **2005**, *101*, 1493.

[38] M. Richert, R. Storandt, *US Patent 4336956*, **1980**.

[39] D. D. Perrin, W. L. F. Armarego, *Purification of Laboratory Chemicals*, Pergamon, New York **1988**.

[40] S. Nygaard, K. C.-F. Leung, I. Aprahamian, T. Ikeda, S. Saha, B. W. Laursen, S.-Y. Kim, S. W. Hansen, P. C. Stein, A. H. Flood, J. F. Stoddart, J. O. Jeppesen, *J. Am. Chem. Soc.* **2007**, *129*, 960.

[41] M. J. Fuchter, L. S. Beall, S. M. Baum, A. G. Montalban, E. G. Sakellariou, N. S. Mani, T. Miller, B. J. Vesper, A. J. P. White, D. J. Williams, A. G. M. Barrett, B. M. Hoffman, *Tetrahedron* **2005**, *61*, 6115.

[42] S. Nygaard, C. N. Hansen, J. O. Jeppesen, *J. Org. Chem.*, DOI: 10.1021/jo061962c.

[43] Fast degradation of the isolated compound **11** was observed, and therefore no further purification was conducted.

[44] The initially interlocked molecule $\mathbf{1}^{4+}$ was left in the doubly oxidized state for a minimum of 39 min in order to create the doubly oxidized linear state $\mathbf{2}^{6+}$.